

# Application of Seismic Wave Method in Early Estimation of Wencheng Earthquake

Wenlong Liu and Yucheng Liu

**Abstract**—This paper introduces the application of seismic wave method in earthquake prediction and early estimation. The advantages of the seismic wave method over the traditional earthquake prediction method are demonstrated. An example is presented in this study to show the accuracy and efficiency of using the seismic wave method in predicting a medium-sized earthquake swarm occurred in Wencheng, Zhejiang, China. By applying this method, correct predictions were made on the day after this earthquake swarm started and the day the maximum earthquake occurred, which provided scientific bases for governmental decision-making.

**Keywords**—earthquake prediction, earthquake swarm, seismic activity method, seismic wave method, Wencheng earthquake

## I. BACKGROUND

CHINESE earthquake researchers started to develop a systematic earthquake prediction methodology after Xingtai earthquake, 1966. Till mid 90's, an appropriate earthquake prediction system was developed and reliable empirical prediction method and criterion were created. Significant progresses have been made in the field of earthquake prediction: at present, medium and long-term earthquake predictions are reliable [1]; 50-year Chinese seismic zoning map have been plotted, which provides an important basis for national land planning and construction; 10 to 15-year key regions of earthquake monitoring and defense have been determined, which is essential to earthquake prevention and disaster reduction; moreover, Chinese earthquake researchers accurately predict the Haicheng earthquake (M7.3) that occurred on February 4, 1975. It is the first successful earthquake forecast in human history and was highly praised by the Chinese government.

Nevertheless, the earthquake prediction comes to a bottle neck at current phase: the accurate rate of year-based medium-term prediction has long been severely varying around 30%; the rate is even lower for short-term forecast, which is only about 10%. Meanwhile, the short-term forecast is only available for a few earthquakes that have foreshock sequence [1]. Advanced prediction method and theory have to be found in order to improve the accuracy of the short-term earthquake prediction.

Professor Wenlong Liu is with the Shanghai Earthquake Administration, Shanghai, China (e-mail: wlliu\_99@yahoo.com).

Professor Yucheng Liu is with the Department of Mechanical Engineering, University of Louisiana at Lafayette, Lafayette, LA 70504, USA. (tel: (337)4825822, fax: (337)482-1129, e-mail: yucheng.liu@louisiana.edu).

Currently, seismic activity method is the most popular method and has been extensively applied in predicting earthquakes, especially in judging the earthquake type and predicting strong aftershocks after strong earthquakes occurred. The seismic activity method is to analyze the time, space, and magnitude of the small and medium earthquakes that occurred before the past strong earthquakes and use these data to predict the future medium and strong earthquakes [2-4]. Therefore, the seismic activity method is an empirical and probabilistic method, which basically belongs to statistical method. To successfully employ the seismic activity method, two conditions have to be satisfied: (1) according to the law of large numbers, the application of this method requires a certain number of previous earthquake samples, the more samples have been analyzed, the higher accuracy can be acquired in predicting the future earthquakes. (2) The earthquake samples have to be complete, and records of all the earthquakes that reached the lowest magnitude have to be kept. Unfortunately, the second condition cannot be fully satisfied, which badly affect accuracy of the short and medium-term predictions. In order to overcome the defects in the current seismic activity method, a new prediction method has to be found in order to improve the fidelity of the earthquake predictions.

## II. SEISMIC WAVE METHOD

### A. Introduction

There is another useful earthquake prediction method called seismic wave method. Seismic waves are waves that travel through the earth as the result of an earthquake. The seismic wave method is to predict the future earthquakes based on the information of stress and medium characteristics at the hypocenter, which are extracted from the seismic waves. This method has aroused a lot of seismologists' interests because of its clear physical meaning and such method is easy for quantification [5-8]. Important parameters and techniques in applying such method are wave-velocity ratio, coda waves and S-waves splitting and polarization. Other descriptive parameters include the hypocenter's dynamic parameters (stress drop  $\Delta\sigma$ , ambient shear stress  $\tau_0$ , and radius of fracture surface  $a$ ), the medium's quality factor  $Q$ , consistency of group identity of the small seismic wave, frequency component, waveform's temporal and spatial linearity, the small earthquake's rupture characteristics ( $L_0/L$ ) [9], and primary rupture direction. In the past, the seismic wave method could not be applied in the earthquake prediction due to the low precision of the previous analog records. However, compare to the mentioned seismic activity method, the seismic wave

method is basically a physical method that requires neither quantity of earthquake samples nor the completeness of those samples. Therefore, this method overcomes the primary flaw of the seismic activity method and has a broad prospect in the earthquake predictions.

### B. Rupture characteristics of medium and small earthquakes

Earthquake's rupture characteristics include unilateral rupture or bilateral rupture, and the primary rupture direction for unilateral rupture. Liu et al [19] presented directional function method to determine the earthquake's rupture characteristics, which is described as follows.

Considering an asymmetric bilateral rupture (Fig. 1), whose rupture propagation velocity is  $v_f$ , rupture lengths of two sides are  $L_0$  and  $L_\pi$ , focal depth  $h = 0$ , and the seismic observatory's epicentral distance is  $r$ . The far-field radiation's P-wave spectrum on the seismic observatory is:

$$U_f(\omega) = \frac{m_0}{4\pi\rho v_p^3 r} R_a i\omega G(\omega) e^{\frac{i\omega r}{v_p}} \left( \frac{L_0}{L} e^{-ix_0} \frac{\sin x_0}{x_0} + \frac{L_\pi}{L} e^{-ix_\pi} \frac{\sin x_\pi}{x_\pi} \right) \quad (1)$$

where  $m_0$  is seismic moment,  $v_p$  is the P-wave velocity, and  $R_a$  is radiation pattern factor:

$$x_0 = \frac{\omega L_0}{2} \left( \frac{1}{v_f} - \frac{\cos \theta}{v_p} \right), \quad x_\pi = \frac{\omega L_\pi}{2} \left( \frac{1}{v_f} + \frac{\cos \theta}{v_p} \right), \quad R_a = \sin 2\theta,$$

$$\text{and } L = L_0 + L_\pi \quad (2)$$

If an earthquake was recorded by seismic observatory 1 and 2, and the epicentral distances of the two observatories were equal to each other (as shown in Fig. 1), then the ratio between the amplitude spectrums obtained from the two observatories can be defined using a directional function  $D$ :

$$D = \frac{|U_1(\omega)|}{|U_2(\omega)|} = \frac{\left| e^{-ix_{10}} \sin x_{10} \left( \frac{1}{v_f} + \frac{\cos \theta}{v_p} \right) + e^{-ix_{1\pi}} \sin x_{1\pi} \left( \frac{1}{v_f} - \frac{\cos \theta}{v_p} \right) \right|}{\left| e^{-ix_{20}} \sin x_{20} \left( \frac{1}{v_f} + \frac{\cos \theta}{v_p} \right) + e^{-ix_{2\pi}} \sin x_{2\pi} \left( \frac{1}{v_f} - \frac{\cos \theta}{v_p} \right) \right|} \quad (3)$$

If the field angle between the lines from both observatories to the epicenter is denoted as  $\alpha$  ( $\alpha \neq \pi$ ), then the ratio between the two amplitude spectrums can be defined as a generalized directional function  $D_G$ :

$$D_G = \frac{\left| \sin 2\theta \left( \frac{1}{v_f} + \frac{\cos(\theta + \alpha)}{v_p} \right) \left( \frac{1}{v_f} - \frac{\cos(\theta + \alpha)}{v_p} \right) \right|}{\left| \sin 2(\theta + \alpha) \left( \frac{1}{v_f} + \frac{\cos \theta}{v_p} \right) \left( \frac{1}{v_f} - \frac{\cos \theta}{v_p} \right) \right|} \times \frac{\left| e^{-ix_{10}} \sin x_{10} \left( \frac{1}{v_f} + \frac{\cos \theta}{v_p} \right) + e^{-ix_{1\pi}} \sin x_{1\pi} \left( \frac{1}{v_f} - \frac{\cos \theta}{v_p} \right) \right|}{\left| e^{-ix_{20}} \sin x_{20} \left( \frac{1}{v_f} + \frac{\cos(\theta + \alpha)}{v_p} \right) + e^{-ix_{2\pi}} \sin x_{2\pi} \left( \frac{1}{v_f} - \frac{\cos(\theta + \alpha)}{v_p} \right) \right|} \quad (4)$$

From above equation, it can be found that  $D_G$  is a function of  $\omega$  with parameters  $\alpha$ ,  $L_0/L$ , and  $\theta$ . As shown in Fig. 1,  $\theta$  is the azimuth angle between the observatory station 1 and Y axis;  $\alpha$  is the azimuth angle between the observatory station 2 and the station 1.

In determining the primary rupture direction based on 2 observatories' records, we first measure the field angle  $\alpha$ . Next, we choose 6  $L_0/L$  values from 0.5 to 1.0 with increment 0.1 and

12  $\theta$  values from  $0^\circ$  to  $180^\circ$  with equal increment  $15^\circ$ . Based on these parameters,  $6 \times 12 = 72$  generalized directional function curves can be calculated from Eqn. (4). The calculated curves are then compared with the curve recorded by the observatory 1 to find the closest calculated curve and corresponding  $L_0/L$  and  $\theta$  values. Two candidate primary rupture directions can be obtained by adding/subtracting the  $\theta$  to/from the observatory 1's geographic azimuth, one of which must be the true primary rupture direction. If more than 3 observatories' records are available, we will be able to obtain more than 2 generalized directional functions  $D_G$  and more than 4 candidate primary rupture directions following the same method. These candidate directions and rupture azimuths are counted based on 4 quadrants, and the quadrant where most rupture azimuths are located is selected. The average value of these selected rupture azimuths is then calculated and specified as the earthquake's primary rupture direction.

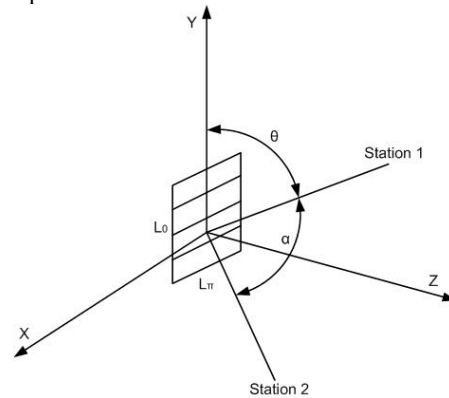


Fig. 1 Asymmetric bilateral rupture

### C. Ambient shear stress

The ambient shear stress values can be determined by employing Chen's method [20, 21]. As declared by Chen et al, by using 2D plane strain crack of mode II to simulate the strike-slip fault and employing rupture mechanics to study the earthquake's rupture process, relationships among the hypocentral parameters and stress conditions can be approximated as:

$$m_s = 2\log(2a) + (\log 4(1 - \nu)\tau^2\eta/3(2 - \nu)\mu - 11.8)/1.5 \quad (5)$$

$$D/2a = 4(1 - \nu)\tau^2/3(2 - \nu)\pi\mu\tau_y \quad (6)$$

$$m_0 = (1 - \nu)\pi\tau^2(2a)^3/3(2 - \nu)\tau_y \quad (7)$$

In Eqns. (5 - 7),  $a$  is the radius of rupture circle,  $\nu$  is the Poisson's ratio (0.252 for the crust),  $\mu$  is the shear modulus (33GPa for the crust),  $\tau$  denotes the ambient shear stress,  $\eta$  denotes the seismic-wave radiation efficiency (we use 0.05 for  $\eta$ ),  $D$  means the average dislocation,  $\tau_y$  is the yield strength (we use 200MPa for the crust),  $m_0$  is seismic moment, and  $m_s$  denotes the surface wave magnitude.

By using dislocation model of circular shear to simulate the medium and small strike-slip earthquakes and taking samples from the seismogram and then performing Fourier analysis, the source spectra can be obtained. From that spectra the spectral amplitude in lower band  $u(\omega)_{\omega \rightarrow 0}$  and corner frequency  $f_{ca}$  can be obtained, therefore the seismic moment  $m_0$  can be determined from:

$$u(\omega)_{\omega \rightarrow 0} = \frac{m_0}{4\pi\rho v_p^3 r} R_\alpha \quad (8)$$

where  $\rho$  is the medium's density (we use  $2.7 \times 10^3 \text{ kg/m}^3$  for the crust),  $r$  is the epicentral distance, the radiation pattern  $R_\alpha = \sin(2\theta)\cos\Phi$  (if  $\theta$  and  $\Phi$  are unknowns, we can take the average radiation pattern calculated over the focal sphere,  $4/15$  for the P wave [22]), and  $v_p$  means P-wave velocity (we assume  $v_p = 5.7 \text{ km/s}$  within the crust [23]). The radius of rupture circle  $a$  can be calculated from the corner frequency  $f_{ca}$  as:

$$f_{ca} = 0.60 / \left[ a \left( \frac{1}{v_f} + \frac{\pi}{4v_p} \right) \right] \quad (9)$$

In above equation, the rupture propagation velocity  $v_f = 0.775v_s$ , where  $v_s$  is S-wave velocity (we assume  $v_s = 3.38 \text{ km/s}$  within the crust [24]). Finally, the ambient shear stress  $\tau$  can be calculated using Eqn. (7) based on  $m_0$  and  $a$ .

#### D. Temporal linearity of waveform

The method of determining temporal linearity waveform  $r$  is illustrated by Feng and Yu [25]. According to their method, a certain number of time  $t_1, t_2, \dots, t_n$  at which the amplitude of displacement or velocity reaches its peak, trough, or zero point are recorded since the P-wave or S-wave first-motion until one or to wave groups end. The time  $t_i$  and the index  $i$  are linearly related:

$$t_i = a + bi \quad (10)$$

where

$$a = [\sum(i \times t_i) \times \sum i - \sum t_i \times \sum i] / [(\sum i)^2 - n \sum(i^2)] \quad (11)$$

$$b = [n \sum(i \times t_i) - \sum t_i \times \sum i \times (i - \sum i / n)] / [(\sum i)^2 - n \sum(i^2)] \quad (12)$$

The errors of  $a$  and  $b$  are:

$$\sigma_a = \sigma_b \sqrt{\sum i^2} / n \quad (13)$$

$$\sigma_b = \left[ \sqrt{\sum \left( t_i - \sum t_i / n \right)^2 \times (n-1)} \right] / \left[ n(n-2) \times \sum \left( i - \sum i / n \right)^2 \right] \quad (14)$$

The temporal linearity of waveform  $r$  is:

$$r = \left\{ \sum \left[ \left( t_i - \sum t_i / n \right) \left( i - \sum i / n \right) \right] \right\} / \left[ \sqrt{\sum \left( t_i - \sum t_i / n \right)^2 \sum \left( i - \sum i / n \right)^2} \right] \quad (15)$$

The more the wave form deviates from the periodic function, the more complicated the rupture process is and the higher unevenness of the medium and stress distributions at the hypocenter, therefore the smaller the  $r$  is.

#### E. Q values for P waves

Assume a seismic observatory has recorded  $n$  earthquakes in one area and the wave spectrum of the  $i$ th earthquake is:

$$Ai(\omega) = Ai_0(\omega)G(Ri)I(\omega)\exp[(-\omega Ri) / (2v_p Q)] \quad (16)$$

In that equation,  $Ai_0(\omega)$  is the seismic wave spectrum from the hypocenter,  $G(Ri)$  is the geometric spreading,  $Ri$  is the hypocentral distance,  $I(\omega)$  is the instrumental frequency characteristic,  $\exp[(-\omega Ri) / (2v_p Q)]$  is the absorption of medium, and  $v_p$  is the P-wave velocity.

In order to determine the  $Q$  value, two frequencies  $\omega_1$  and  $\omega_2$  are substituted into Eqn. (16) to find the frequency ratio:

$$\ln|Ai(\omega_1)/Ai(\omega_2)| = \ln|Ai_0(\omega_1)/Ai_0(\omega_2)| - (\omega_1 - \omega_2)Ri/(2v_p Q) \quad (17)$$

In Eqn. (17),  $(\omega_1 - \omega_2)Ri/(2v_p Q)$  is a constant and

$\ln|Ai_0(\omega_1)/Ai_0(\omega_2)|$  of different recorded earthquakes can also be treated as a constant if these earthquakes occurred in the same area and whose magnitudes were close to each other. Thus, the  $Q$  values can be directly calculated from Eqn. (17).

#### F. Width of Fourier spectrum

The width of Fourier spectrum is defined as the bandwidth which is 70% of the maximum spectral amplitude. A wider Fourier spectrum indicates that the seismic wave has more frequency components, therefore the rupture process should be more complicated and the medium and stress distribute more unevenly at the hypocenter.

#### G. Future application

So far, the maximum depth of physical exploration and drilling is 10km. Therefore, almost 90% of the knowledge about the interior of the earth is obtained from the seismic waves. In most earthquakes, the hypocenter is deeper than 10km beneath the earth crust and the seismic wave thus becomes the only carrier of the hypocentral information. The seismic activity method only uses a little information provided by the seismic wave: P- and S-waves arrival times and amplitudes. In order to improve the earthquake prediction level, the affluent information carried by the seismic wave has to be utilized.

The understanding of mankind to the nature has been improved with the development of the observation and experiment instruments. In last 70's, the seismic activity method was prospered in China with the establishment of Chinese regional analog earthquake monitoring network. The time, space, and magnitude were then determined as the three factors in describing the small and medium-sized earthquakes. At the beginning of the 21<sup>st</sup> Century, Chinese earthquake monitoring mode started to be transferred from the analog recording mode to the digital mode, which is a significant advancement. The analog records only can be used for studying seismic rays while the digital records can also be applied to investigate most information provided by the seismic waves, through which the medium characteristics and the preparation of hypocenter can be revealed. In conclusion, there is a good opportunity to fully develop the seismic wave method based on this technological advancement in order to improve the level of the earthquake predictions. In next section, an illustrative example is presented to demonstrate how to apply the seismic wave method to make correct earthquake forecasts.

### III. EXAMPLE: FORECASTING OF $M_L 4.6$ EARTHQUAKE SWARM IN WENCHENG, ZHEJIANG PROVINCE

#### A. Outline

From 4:46 of February 4<sup>th</sup> 2006, an earthquake swarm with maximum magnitude  $M_L 4.6$  occurred in Wencheng County, Zhejiang Province, and lasted for several months. From February 4<sup>th</sup> to February 14<sup>th</sup>, 2006, overall 1237 earthquakes or shocks occurred, among which 32 earthquakes with  $M_L \geq 3.0$  and 9 earthquakes had  $M_L \geq 4.0$  (see Table 1 and Fig. 2). After February 14<sup>th</sup> till March 10<sup>th</sup>, 2006, 7 earthquakes with magnitude  $\geq 3$  occurred in the same area and the maximum

magnitude is 3.9, which occurred at 15:24 on March 10<sup>th</sup>. The hypocenters of these earthquakes were located within 10km from the earth crust and the minimum distance between the hypocenter and the earth surface was less than 4km. The epicenters of these earthquakes were concentrated at Shanxi reservoir within an area of 5km<sup>2</sup>.

TABLE 1. DAY-TO-DAY FREQUENCY OF EARTHQUAKES WITH  $M_L \geq 1.0$  IN WENCHENG  $M_L 4.6$  EARTHQUAKE SWARM (4:46 FEB 4<sup>th</sup> 2006 TO 14:48 FEB 14<sup>th</sup> 2006)

Date	2/4	2/5	2/6	2/7	2/8	2/9	2/10	2/11	2/12	2/13	2/14
Times	85	43	43	44	108	231	257	156	125	100	45

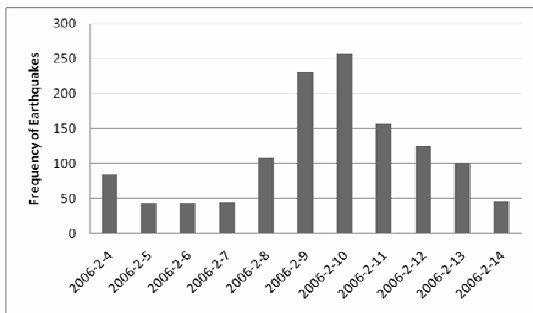


Fig. 2 Frequency of  $M_L \geq 1.0$  earthquakes in Wencheng  $M_L 4.6$  earthquake swarm from Feb 4<sup>th</sup> 2006 to Feb 14<sup>th</sup> 2006)

The Shanxi reservoir is located at (120.05°E, 27.67°N). Height of the reservoir's dam is 156.8m and length of the dam is 308m. The maximum capacity of this reservoir is  $18.24 \times 10^8 \text{ m}^3$  and the reservoir level is 154.75m. According to historical records, 8 earthquakes with  $M_L \geq 4.7$  had occurred in the area centered on the reservoir with radius 50km. The strongest earthquake occurred in 1574 with the magnitude  $M_L 5.5$ , whose epicenter was 86km far from the Shanxi reservoir. From 1971 to 2002, there was no earthquake recorded in this area. The reservoir was founded in 2001 and the first earthquake on this reservoir area occurred on July 28<sup>th</sup>, 2002. Since that time, 207 earthquakes have been monitored and recorded, the magnitude distribution is: 1.0 – 1.9 (80 times), 2.0 – 2.9 (27 times), 3.0 – 3.9 (8 times), and above 4 (2 times) [11].

Because the hypocenters of these earthquakes are close to the earth crust, these earthquakes ( $M_L \geq 2.0$ ) caused a lot of damages in local area. A number of buildings ruptured and a few of them even collapsed. Thousands of people had to live in tents and panic spread over the crowd. Chinese Premier Wen paid highly attention to this disaster and required related units to evaluate these occurred earthquakes and forecast the future trends.

By applying the seismic wave method, we made correct predictions about this earthquake swarm on the next day it started (February 5<sup>th</sup>, 2006) and on the day the strongest earthquake ( $M_L 4.6$ ) occurred (February 9<sup>th</sup>, 2006). More details about the predictions are illustrated in following sections.

#### B. Forecast mode on February 5<sup>th</sup>, 2006

After receiving the earthquake report, the authors make an instant judgment about the future earthquake trends in the morning of February 5<sup>th</sup>, one day after the first earthquake occurred. In that judgment, it was indicated that the

earthquakes happened in February 4<sup>th</sup> belonged to a sequence of small and medium-sized earthquakes, which would last out for a period of time and the maximum magnitude would reach  $M_L 4.5$ . This forecast was made based on following observations and analyses.

- (1) As shown from Table 2 and Fig. 3, 6 earthquakes with magnitude  $M_L$  above 3.0 occurred on February 4<sup>th</sup>. Their magnitudes were 3.5, 3.0, 3.7, 4.0, 3.1, and 4.1, according to the time they occurred. These six earthquakes accompanied by concentrated small earthquakes can be divided into three groups based on their occurring times, with time space about 5 hours. From the listed data, it could be deduced that the magnitudes of these earthquakes were ascending. After the time that the last medium-sized earthquake ( $M_L 4.1$ ) occurred till February 5<sup>th</sup> morning (10 am), there was no medium-sized earthquake ( $M_L \geq 3.0$ ) reported, despite of scattered small earthquakes. These data indicated that the first sequence of earthquakes started on February 4<sup>th</sup> went into the end but might be followed with stronger earthquakes.

TABLE II CATALOG OF EARTHQUAKES WITH  $M_L \geq 3.0$  IN WENCHENG  $M_L 4.6$  EARTHQUAKE SWARM

Date	2-4	2-4	2-4	2-4	2-4	2-4	2-7	2-8	2-8	2-8
Time	04:46	05:24	05:55	11:13	16:18	16:52	19:26	01:26	01:29	03:38
$M_L$	3.5	3.0	3.7	4.0	3.1	4.1	3.6	3.0	4.4	3.1
Date	2-9	2-9	2-9	2-9	2-9	2-9	2-9	2-9	2-9	2-10
Time	03:24	03:25	03:27	03:45	09:36	10:53	17:09	17:11	18:51	02:45
$M_L$	4.6	3.4	4.1	3.6	3.7	3.7	3.0	3.3	4.2	3.2
Date	2-10	2-10	2-10	2-11	2-11	2-11	2-11	2-11	2-12	2-12
Time	07:59	13:46	14:37	04:36	05:05	09:11	16:36	22:01	05:15	10:33
$M_L$	4.2	3.3	4.1	4.2	3.8	3.0	3.0	3.2	3.1	3.7
Date	2-12	2-12	2-14	2-20	2-25	3-4	3-6	3-10	3-10	
Time	20:16	21:55	19:40	15:22	03:45	02:02	09:23	15:24	15:35	
$M_L$	3.3	3.2	3.2	3.8	3.1	3.2	3.7	3.9	3.8	

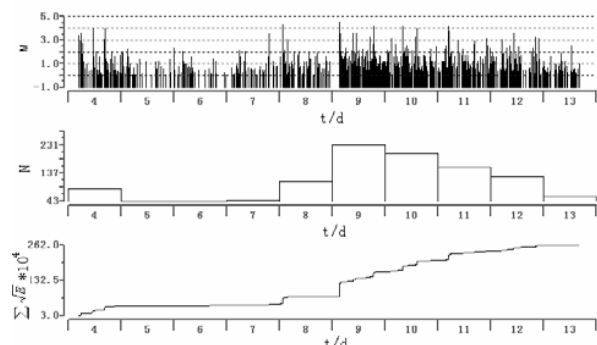


Fig. 3 M-T, N-T, and  $\sum \sqrt{E}$  -T plots for Wencheng  $M_L 4.6$  earthquake swarm in Feb-2006 [10]

- (2) As introduced before, in this area, there has been no fracture caused by seismic activities reported since Neogene. Also there was no earthquake with  $M_L$  above 4.8 recorded in the area within 50km from the epicenter in history. Moreover, from 1971, when monitoring instruments were firstly put to use in this area, till year 2002, even no earthquake was detected. Meanwhile, based on current data, there wasn't any abnormalities

detected that could induce the damaging earthquake with magnitude above 5.0. Therefore, the probability of having earthquake with  $M_L \geq 5.0$  in the future is very low.

- (3) Shanxi reservoir was put to use in May of 2000 and the first earthquake in this reservoir area occurred on July 28<sup>th</sup>, 2002, which belonged to a small earthquake swarm. Before the Wencheng  $M_L 4.6$  earthquake, the maximum earthquake in the area occurred on September 5<sup>th</sup>, 2002 with magnitude  $M_L = 3.9$ . Thus, the earthquakes occurred on February 4<sup>th</sup>, 2006 must also belong to a sequence of small earthquake swarm. Based on statistics, in an earthquake swarm sequence, the magnitude difference between the largest and the second largest earthquakes are within 0.6 [12]. Therefore, if  $M_L 4.1$  was the magnitude of the second largest earthquake in this sequence, the maximum magnitude of future earthquake would not exceed  $M_L 4.7$ , and should be around  $M_L 4.5$ .
- (4) The maximum magnitude of the earthquakes induced by reservoir depends on the scale of the reservoir and can be evaluated as [13]:

$$M = 1.317 + 0.995E \pm 1.201 \quad (18)$$

where  $M$  is the maximum magnitude of the earthquake induced by the reservoir,  $E$  is a general impact coefficient, which equals:

$$E = S \times H_{\max} / V \quad (19)$$

where  $S$  is the area of the reservoir,  $H_{\max}$  is the depth of the reservoir before its dam, and  $V$  is the reservoir's capacity. In Shanxi reservoir, its overall area is  $34.1 \text{ km}^2$ ,  $H_{\max}$  is  $129.75 \text{ m}$ , and its capacity is  $18.24 \times 10^8 \text{ m}^3$ . By using Eqns. (18) and (19), the maximum magnitude in this earthquake swarm could be predicted as  $M_L 4.5$ .

### C. Forecast mode on February 9<sup>th</sup> and February 12<sup>th</sup>, 2006

On February 9<sup>th</sup>, 2006, after knowing the  $M_L 4.6$  earthquake occurred (Table 2), we instantly estimated that it should be the maximum earthquake in this earthquake swarm. This judgment was made based on two reasons: 1) empirically, the maximum earthquake in an earthquake swarm always occurs in the prophase of the second sequence of earthquakes; 2) the reported magnitude  $M_L 4.6$  was close to our estimated maximum magnitude value. This hypothesis was subsequently verified by using the seismic wave method.

We arrived at the earthquake scene at February 12<sup>th</sup> morning and collected all data recorded by local observatories. After thoroughly analyzing these materials and data, the final forecasts were made and submitted to related governmental sections. In these forecasts, it was declared that: 1) the earthquakes initiated on February 4<sup>th</sup> are earthquake swarm activities instead of being a sequence of foreshock; 2)  $M_L 4.6$  earthquake occurred on February 9<sup>th</sup> was the maximum earthquake in this earthquake swarm. These earthquake activities might last out for a period of time and even be accompanied with medium-sized earthquakes with magnitude around  $M_L 4.0$ . However, the magnitudes of the future earthquakes would not exceed  $M_L 4.6$ . Our reasons are:

- (1) From Fig. 3 and Table 2, it can be found that after the  $M_L 4.6$  earthquake occurred on February 9<sup>th</sup> till February 12<sup>th</sup> 22:00, overall 21 earthquakes with  $M_L \geq 3.0$  occurred, among which 5 earthquakes had the magnitude  $M_L \geq 4.0$ . The time intervals between these medium-sized earthquakes obviously increased and the magnitudes of these earthquakes were generally in a descending trend. The last earthquake with  $M_L \geq 4.0$  occurred at 4:36 on February 11<sup>th</sup> ( $M_L 4.2$ ) and since then there was no such earthquake ( $M_L \geq 4.0$ ) occurred till 22:00 February 12<sup>th</sup>, when our forecasts were made. Meanwhile, the frequency of occurrence of the small earthquakes also decayed in this period of time. These phenomena suggested that the  $M_L 4.6$  earthquake should be the maximum earthquake in this earthquake swarm.
- (2) After the  $M_L 4.6$  earthquake, apparent variations were observed from the seismic waveforms of the  $M_L \geq 3.0$  earthquakes, which had been recorded by a local observatory, Wenzhou seismic station. As shown in Fig. 4, the amplitude ratio  $A_S/A_P$  (which means the ratio between the maximum amplitude of S-wave and P-wave) was consistent before the  $M_L 4.6$  earthquake on February 9<sup>th</sup>. Most  $A_S/A_P$  values before February 9<sup>th</sup> were close to 5, except for the  $M_L 3.6$  earthquake occurred at 19:26 February 7<sup>th</sup>, whose  $A_S/A_P$  was 16.85. However, this ratio significantly dispersed after the  $M_L 4.6$  earthquake. As displayed in Fig. 4, numerically, these discrete values can be evenly divided into three groups: around 5; around 10; and between 15 and 20.

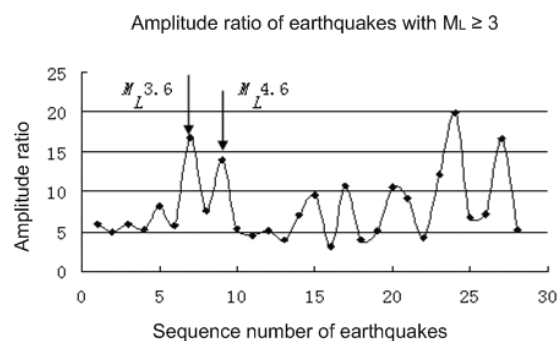


Fig. 4  $A_S/A_P$  plots of Wencheng  $M_L 4.6$  earthquake swarm, recorded by Wenzhou seismic station [10]

Fig. 5 shows the rising times of P-wave initial motions of these  $M_L \geq 3.0$  earthquakes. From that figure, it can be found that the rising times of the earthquakes that occurred before the  $M_L 4.6$  earthquake were all less than 0.12 second. After the  $M_L 4.6$  earthquake, a number of earthquakes occurred, whose P-wave initial motion's rising time was longer than 0.12 second. The increase of the P wave's rising time implied that the stress released from per unit fracture surface was decreased, and the level of ambient shear stress was also reduced. Therefore, the magnitude of future earthquakes would not exceed  $M_L 4.6$ .

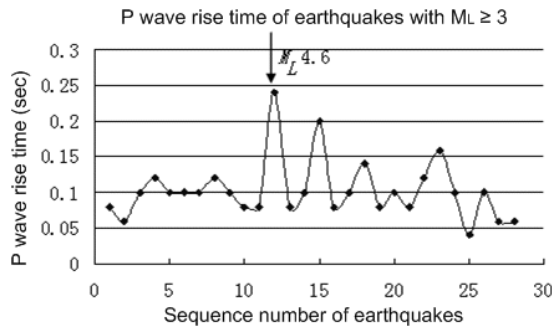


Fig. 5 P wave's rising time of Wencheng  $M_L 4.6$  earthquake swarm, recorded by Wenzhou earthquake station [10]

These forecasts were made on February 12<sup>th</sup>, 2006 and the subsequent records (Table 2) fully verified accuracy of our forecasts.

#### D. The factor that caused Wencheng earthquake swarm

Another important factor that affects the sequence of small earthquake occurrence is the water level of the reservoir. Niu et al [18] analyzed this Wencheng earthquake and demonstrated cause of this earthquake and the correlations of earthquake occurrence time and the reservoir level changes and tides. Since this reservoir was put to use in May 2000, there are 4 periods of time that the Shanxi reservoir water level remains high. Those time periods are: May 2002 ~ September 2002 (max. 135.7m); May 2003 ~ September 2003 (max. 134m); September 2004 ~ December 2004 (max. 140.2m); May 2005 ~ November 2005 (max. 145.2m). 6 small earthquake swarms occurred after its impoundment, these earthquake swarms are: July-28-2002 ~ November-29-2002, 46 small earthquakes, the maximum one occurred on September 5 with magnitude  $M_L 3.9$ ; May-2-2003 ~ October-7-2003, 20 small earthquakes and the maximum one occurred on September 13 with  $M_L 1.9$ ; January-11-2004 ~ April-10-2004, 16 small earthquakes, the maximum earthquake  $M_L 1.5$  occurred on February 1; December-29-2004 ~ March-24-2005, 69 small earthquakes and the maximum one  $M_L 2.2$  occurred on January 22; August-27-2005 ~ December-27-2005, 13 small earthquakes, with the maximum one  $M_L 2.1$  occurred on August 27; and this Wencheng  $M_L 4.6$  earthquake swarm.

From 1971 to 2002, there was no earthquake recorded in this area and the small earthquakes only occurred within the few years after this reservoir impoundment. It is well known that the water level of the dam reservoir affects the small earthquake activities and the change in water level may increase level of seismicity. Table 3 shows the correlations between the water level and the occurrence of small earthquake swarms.

TABLE III. SHANXI RESERVOIR'S WATER LEVEL AND OCCURRENCE OF SMALL EARTHQUAKE SWARMS

No.	1	2	3	4
Water level	05-09 2002	05-09 2003	09-12 2004	05-11 2005
Peak level	135.7m	134m	140.2m	145.3m
Small earthquake swarm	7-28-02 ~ 11-29-02	5-2-03 ~ 10-7-03	1-11-04 ~ 3-24-05	8-27-05 ~ 12-27-05
frequency	46	20	16	69
Max. magnitude	$M_L 3.9$ (9-5-02)	$M_L 1.9$ (9-13-03)	$M_L 1.5$ (2-1-04)	$M_L 2.2$ (1-22-05)
				$M_L 2.1$ (8-27-05)
				$M_L 4.6$

From table 3, it can be found that the first two small earthquake swarms were induced by the high water level in the first duration; the third and fourth earthquake swarms were induced by the high water level in the second and third durations, respectively; and the last two earthquake swarms were induced by the high water level in the fourth duration. Several observations can be made from that table:

- (1) Small earthquake swarms usually occurred during discharging processes, where the water level decreased after reaching the peak levels.
- (2) The reservoir induced earthquakes occurred within the few years after the reservoir impounding and attenuated along with time. Such characteristics can be observed from the first to fifth earthquake swarms listed in table 3. For example, the water level in the third time period (140.2m) is higher than the first one (135.7m), but the maximum magnitude of the induced earthquake in that period ( $M_L 2.2$ ) is lower than the one in the first time period ( $M_L 3.9$ ).
- (3) In two consecutive time periods, the magnitude and frequency of the small earthquakes is proportional to the water level, which can be observed by comparing the second and third durations of high water level.

This  $M_L 4.6$  earthquake swarm occurred after the fourth duration of high water level, which was also caused by the change of the reservoir's water level. However, the activity and magnitude of this earthquake swarm are by far higher than the five previous earthquake swarms, which can not be attributed to the reservoir's effects but the change of the local stress field.

Since middle of 1990s, the medium and small earthquake activities have been escalating in southeastern China (the area to the south of 34° North Latitude). Since the occurrences of  $M_s 6.1$  earthquake on November-9-1996 in the east of Yangtze River estuary and  $M_s 5.3$  earthquake on July-28-1997 in southern Yellow Sea, the earthquake activity in this area underwent three phases. 1) During 1998 ~ 2001, the medium and small earthquake activities continuously decreased, which showed that this area was in a process of stress adjustment after the  $M_s 6.1$  and  $M_s 5.3$  earthquakes. 2) In 2002 and 2003, the medium and small earthquake activities slowly increased, which reflected that this area was in another process of stress intensification. 3) Since April of 2004 till now the medium and small earthquake activities obviously increased. A number of  $M_L \geq 3.0$  earthquakes occurred in this area and the strongest earthquake is  $M_L 4.7$  that occurred on November-15-2004 in southern Yellow Sea (32°30', 123°40'). It indicates an accelerating stress accumulation in this area. Table 4 lists the

occurrence of medium and small earthquakes occurred in southern Yellow Sea and its coastal regions in recent years.

TABLE IV. FREQUENCY OF EARTHQUAKES IN SOUTHERN YELLOW SEA AND ITS COASTAL REGIONS

Year	Magnitude					Energy released (kJ)
	$M_L \geq 2.0$	$M_L \geq 3.0$	$M_L \geq 4.0$	$M_L \geq 5.0$	$M_L \geq 6.0$	
1997	42	14	5	2	1	$1.12 \times 10^{11}$
1998	46	12	2	0	0	$1.28 \times 10^8$
1999	38	10	1	0	0	$6.14 \times 10^7$
2000	39	8	0	0	0	$1.52 \times 10^7$
2001	41	4	0	0	0	$5.58 \times 10^6$
2002	58	6	0	0	0	$1.62 \times 10^7$
2003	40	8	0	0	0	$3.91 \times 10^6$
2004	49	11	1	0	0	$2.07 \times 10^8$
2005	46	8	1	0	0	$1.58 \times 10^8$
Average	37.08	9.04	1.24	0.56	0.12	$1.02 \times 10^{10}$

In summary, the Wencheng  $M_L 4.6$  earthquake swarm was not only triggered by the reservoir's water lever but also a result of accumulation of stress in this local area. Thus, this Wencheng  $M_L 4.6$  earthquake swarm required us to pay attention to the southern Yellow Sea and its coastal regions, especially the area to the south of  $34^\circ$  North Latitude and analyze the possibility of having medium and strong earthquakes in that area.

#### IV. DISCUSSION

There were some experts argued against our conclusions and insisted that stronger earthquakes (with  $M_L \geq 4.6$ ) would occur in the future because the  $b$  and  $h$  values of this earthquake sequence were very low. In fact, till February 13<sup>th</sup>, this sequence's  $b = 0.56$  and  $h = 0.1$ , both of them were much lower than 1. In the traditional seismic activity method [14] and according to modified Omori's law and Utsu's theories [15-17], the low  $b$  and  $h$  values measured in an ongoing earthquake sequence indicates the occurrence of stronger earthquakes in the future. However, these  $b$  and  $h$  values were calculated during the period from February 4<sup>th</sup>, the starting time of this earthquake sequence, to February 13<sup>th</sup>. If we selected the period from February 9<sup>th</sup>, right after the  $M_L 4.6$  earthquake occurred, to February 13<sup>th</sup> and re-calculated  $b$  and  $h$ , we would have  $b = 0.59$  and  $h = 0.98$ . From the comparison, it can be found that after the  $M_L 4.6$  earthquake, both  $b$  and  $h$  values increased, especially the  $h$  value, which significantly increased to almost 1. Meanwhile, in this case, the comparatively low  $b$  and  $h$  values were caused by the features of this earthquake sequence, such as the long lasting time, the slow attenuation, and the large undulation in the magnitudes of these earthquakes.

Since this paper was finished, till now there has no earthquake of  $M_L \geq 4.6$  occurred in this area and the strongest earthquake is  $M_L 4.5$ , which occurred at 14:07 on August-1-2005. This fact again verified our conclusion.

#### V. CONCLUSION

In this study, the seismic wave method is introduced and successfully applied to predict the Wencheng  $M_L 4.6$

earthquake swarm. By using this method, we concluded that the maximum magnitude of this earthquake swarm is  $M_L 4.6$  and this small earthquake swarm was caused by the change of water level of Shanxi reservoir and the change of local area's stress field. Our predictions were then documented and reported to the government of Zhejiang Province, which played a decisive role in the government's decision-making. Earthquake reports made thereafter fully verified our judgments. This illustrative example shows that the seismic wave method is capable of quickly and correctly making forecasts on earthquakes or earthquake swarms therefore has a broad prospect in earthquake prediction. Specifically, in its future application, special attentions need to be paid to following points:

- (1) Error estimation should be given along with the earthquake predictions in order to make the predictions more convincing.
- (2) The seismic wave method can be combined with the seismic activity method in applying for predicting individual foreshocks and rapid determination of the earthquake trends and type after strong earthquakes.
- (3) In current phase, it is very important to apply the seismic wave method to study as many earthquake examples as possible. A complete set of samples need to be collected to guarantee the reliability of this method.
- (4) The occurrence of the earthquake and the type of the earthquake sequence are mainly caused by the unevenness of distribution of the earth stress and the characteristics of the medium. Therefore it must be helpful to find representative parameters that can reflect the unevenness of the stress distribution and medium characteristics at the hypocenter.
- (5) In order to improve the accuracy of the earthquake prediction (especially the short-term prediction), the earthquake prediction mode should be transferred from the statistical mode to the physical mode. The traditional empirical method should be integrated with the earthquake preparation theory and the ultimate goal of the seismic wave method is to develop a physical model that can correctly describe the gestation and generation of the earthquake, through which the accurate earthquake prediction can be achieved.

#### REFERENCES

- [1] G. O. Young, "Synthetic structure of industrial plastics (Book style with paper title and editor)," in *Plastics*, 2nd ed. vol. 3, J. Peters, Ed. New York: McGraw-Hill, 1964, pp. 15-64.
- [2] G.-M. Zhang, "The main science advance of earthquake monitoring and prediction in China", *Earthquake*, 22(1), 2002, 26-31 (in Chinese)
- [3] V.G. Kossobokov, J.H. Healy, J.W. Dewey, "Testing an earthquake prediction algorithm", *Pure and Applied Geophysics*, 149(1), 1997, 219-232
- [4] D.L. Turcotte, "Earthquake prediction", *Annual Review of Earth and Planetary Sciences*, 19, 1991, 263-281
- [5] V.I. Keilis-Borok, A.A. Soloviev, *Nonlinear Dynamics of the Lithosphere and Earthquake Prediction*, Springer, 2003
- [6] J. Gombert, P.A. Reasenber, P. Bodin, R.A. Harris, "Earthquake triggering by seismic waves following the Landers and Hector Mine earthquakes", *Nature*, 411, 2001, 462-466
- [7] Y. Tanioka, K. Satake, "Detailed coseismic slip distribution of the 1944 Tonankai earthquake estimated from tsunami waveforms", *Geophysical Research Letters*, 28(6), 2001, 1075-1078

- [8] S. Gao, H. Liu, P.M. Davis, L. Knopoff, "Localized amplification of seismic waves and correlation with damage due to the Northridge earthquake: evidence for focusing in Santa Monica", *Bulletin of the Seismological Society of America*, 86, 1996, S209-S230
- [9] H. Sato, M.C. Fehler, *Seismic Wave Propagation and Scattering in the Heterogeneous Earth*, Springer Berlin Heidelberg, 2009
- [10] W.-L. Liu and P.-Z. Wu, "Fracture feature determination of an earthquake by using the directional function", *Earthquake Research in China*, 12(1), 1996, 93-99 (in Chinese)
- [11] W.-L. Liu and H.-Y. Yu, "Spot forecast of the ML4.6 earthquake swarm of Shanxi reservoir, Zhejiang Province occurred on Feb. 9, 2006", *South China Journal of Seismology*, 26(3), 2006, 34-44 (in Chinese)
- [12] Y.-Y. Zhong, F. Zhang, and Z.-F. Zhang, "Wenzhou Shanxi reservoir induced earthquake research", *Geodesy and Geodynamics*, 25, 2005, 26-31 (in Chinese)
- [13] Y.-Z. Lu, Z.-L. Chen, B.-Q. Wang, P.-X. Liu, W.-L. Liu, and W.-L. Dai, *Seismic earthquake prediction method*, Earthquake Press, Beijing, 1985, Chapter 3 (in Chinese)
- [14] Y.-Z. Ding, B.-Q. Chang, X.-A. Yu, *Reservoir induced earthquake*, Earthquake Press, Beijing, 1989, 154-155 (in Chinese)
- [15] Z.-R. Liu, Z.-X. Qian, H.-Q. Wang, "An indication of foreshocks – seismic decay" *Journal of Seismological Research*, 2(4), 1979, 1-9 (in Chinese)
- [16] T. Utsu, "A method for determining the value of b in a formula  $\log n = a - bM$  showing the magnitude-frequency relation for earthquakes", *Geophysics Bulletin of Hokkaido University*, 13, 1965, 99-103 (in Japanese)
- [17] T. Utsu, "Statistical significance of test of the difference in b value between two earthquake groups", *Journal of Physics of the Earth*, 14, 1974, 37-40
- [18] T. Utsu, Y. Ogata, and R. S. Matsu'ura, "The centenary of the Omori formula for a decay law of aftershock activity", *Journal of Physics of the Earth*, 43, 1995, 1-33
- [19] A.-F. Niu, X.-D. Zhang, D.-L. Zheng, X.-F. Li, P. Ji, "On the occurrence time of an earthquake cluster", *Earthquake Research in China*, 20(4), 2006, 406-411
- [20] W.-L. Liu, P.-Z. Wu, Y.-W. Chen, "Determination of earthquake's rupture characteristics using directional function", *Earthquake Research in China*, 1996 12(1), pp.93-99
- [21] P.-S. Chen, J.-C. Gu, W.-X. Li, "Study of earthquake's rupture process and prediction applying rupture mechanics", *Chinese Journal of Geophysics*, 1977 20(3), pp. 185-201
- [22] P.-S. Chen, Y.-R. Zhuo, Y. Jin, Z.-G. Wang, W.-Q. Huang, W.-X. Li, R.-S. Hu, "Stress field of Beijing, Tianjin, Tangshan, and Zhangjiakou area before and after Tangshan earthquake", *Chinese Journal of Geophysics*, 1978 21(1), pp. 24-58
- [23] A. Venkataraman, "Investigating the mechanics of earthquakes using macroscopic seismic parameters", *Doctorate Thesis*, California Institute of Technology, Pasadena, California, 2002
- [24] T. Lidaka, A. Kato, E. Kurashimo, T. Iwasaki, N. Hirata, H. Katao, I. Hirose, H. Miyamachi, "Fine structure of P-wave velocity distribution along the Atotsugawa fault, central Japan", *Tectonophysics*, 2009 472(1-4), pp. 95-104
- [25] F.T. Wu, A.L. Levshin, V.M. Kozhevnikov, "Rayleigh wave group velocity tomography of Siberia, China and the Vicinity", *Pure and Applied Geophysics*, 1997 149(3), pp. 447-473
- [26] D.-Y. Feng, X.-J. Yu, "Application of seismic wave's dynamic characteristics in short term earthquake prediction", *Earthquake*, 1994 1, pp. 12-22

**Professor Wenlong Liu** graduated from University of Science and Technology of China in 1970. Professor Liu is the Full Professor of Shanghai Earthquake Administration and holds the Professorship at University of Science and Technology of China. Professor Liu is also the Chinese National Seismic Safety Evaluation Engineer. During his 40-year career of earthquake prediction and seismology, he served as the Director of Anhui Earthquake Prediction and Research Center, Director of Shanghai Earthquake Prediction Institute, the Chief Scientist of Shanghai Earthquake Administration, and the Senior Scientist of China Earthquake Administration. Professor Liu serves on diverse panels and committees, including the panel of Chinese National Science Foundation (NSF); the awards committee of Chinese Science and Technology Progress Award; and the awards committee of Shanghai Science and Technology Progress Award. Professor Liu is also a recipient of the Chinese State Department Special Government Allowances.

Professor Liu's significant contributions include: creating the short and medium-term forecasting system to predict earthquakes in eastern China and its adjacent sea area; developing the method of early judgement of the earthquake trends after an earthquake; developing the method to predict the strong aftershock; presenting the directional function method to determine the rupture characteristics of small and medium-size earthquakes; discovering the rupture characteristics of seismic gap during a foreshock or an earthquake that occurs in the seismic zone; determination of the coda wave attenuation coefficient and discovering its varying characteristics before medium-size and strong earthquakes; constructing the physical model for the local internal stress of earthquake; discovering that in an earthquake sequence, the small-size earthquakes have identical initial motion direction before the maximum earthquake and this direction turns to turbulence after the maximum earthquake. Professor Liu achieved following accomplishment as a principle investigator: construction of the Shanghai digital earthquake precursor network; construction of the earthquake prediction system in Anhui Province. He is also the leading author of the annual reports of seismic trend research in eastern China from year 1988 to 2005.

**Dr. Yucheng Liu** is an Assistant Professor of Mechanical Engineering at University of Louisiana at Lafayette. Dr. Liu received his PhD degree from the University of Louisville in 2005. Dr. Liu's research interests include structural mechanics and dynamics, applied mathematics, etc. To date, he has about 50 publications (books, journal articles, and conference proceedings) in his areas. Dr. Liu is an editorial member of a refereed journal and has reviewed papers for 13 journals and 4 conferences. Dr. Liu is a member of WASET Scientific and Technical Committee on Natural and Applied Sciences. He is also a Professional Engineering registered in Ohio, USA and holds membership in ASME and SAE.